A close-ring pair terahertz metamaterial resonating at normal incidence

Jianqiang Gu[1,2], Jiaguang Han[3], Xinchao Lu[1], Ranjan Singh[1], Zhen Tian[1,2], Qirong Xing[2], and Weili Zhang[1,*]

[1]*School of electrical and computer Engineering, Oklahoma State University, Oklahoma 74078*
[2]*Center for Terahertz Waves, College of Precision Instrument & Optoelectronics Engineering, and Key Lab of Opto-electronics Information and Technical Science (Ministry of Education), Tianjin University, Tianjin 300072, China*
[3]*Department of Physics, National University of Singapore, 2 Science Drive 3, Singapore 117542*
**weili.zhang@okstate.edu*

Abstract: We present a systematic study of a close-ring pair based freestanding metamaterial fabricated by double-layer, self-aligned photolithography. Terahertz time-domain spectroscopy transmission measurements and numerical simulations have revealed negative index of refraction in the frequency range of 0.66-0.90 THz under normal wave incidence. The observed resonance behaviors can be well explained by a theoretical circuit model. The electromagnetic properties and the figure of merit of such close-ring metamaterials are also explored in terms of geometrical parameters of the unit cell with a goal of providing optimized design for three-dimensional metamaterials and potential device applications.

OCIS codes: (160.3918) Metamaterials; (260.5740) Resonance

References and links

1. V. G. Veselago, "The Electrodynamics of Substances with Simultaneously Negative Values of ε and μ," Sov. Phys. Usp. **10**, 509 (1968).
2. N. Fang, H. Lee, C. Sun, and X. Zhang, "Sub-Diffraction-Limited Optical Imaging with a Silver Superlens," Science **308**(5721), 534–537 (2005).
3. D. Schurig, J. J. Mock, B. J. Justice, S. A. Cummer, J. B. Pendry, A. F. Starr, and D. R. Smith, "Metamaterial Electromagnetic Cloak at Microwave Frequencies," Science **314**(5801), 977–980 (2006).
4. T. J. Yen, W. J. Padilla, N. Fang, D. C. Vier, D. R. Smith, J. B. Pendry, D. N. Basov, and X. Zhang, "Terahertz Magnetic Response from Artificial Materials," Science **303**(5663), 1494–1496 (2004).
5. M. W. Klein, C. Enkrich, M. Wegener, and S. Linden, "Second-Harmonic Generation from Magnetic Metamaterials," Science **313**(5786), 502–504 (2006).
6. R. W. Ziolkowski, and A. Erentok, "Metamaterial-based efficient electrically small antennas," IEEE Trans. Antenn. Propag. **54**(7), 2113–2130 (2006).
7. H. T. Chen, W. J. Padilla, J. M. O. Zide, A. C. Gossard, A. J. Taylor, and R. D. Averitt, "Active terahertz metamaterial devices," Nature **444**(7119), 597–600 (2006).
8. T. Xu, Y. Zhao, J. Ma, C. Wang, J. Cui, C. Du, and X. Luo, "Sub-diffraction-limited interference photolithography with metamaterials," Opt. Express **16**(18), 13579–13584 (2008).
9. J. F. O'Hara, R. Singh, I. Brener, E. Smirnova, J. Han, A. J. Taylor, and W. Zhang, "Thin-film sensing with planar terahertz metamaterials: sensitivity and limitations," Opt. Express **16**(3), 1786–1795 (2008).
10. R. Singh, C. Rockstuhl, C. Menzel, T. P. Meyrath, M. He, H. Giessen, F. Lederer, and W. Zhang, "Spiral-type terahertz antennas and the manifestation of the Mushiake principle," Opt. Express **17**(12), 9971–9980 (2009).
11. B. Wood, and J. B. Pendry, "Magnetism from conductors and enhanced nonlinear phenomena," IEEE Trans. Microw. Theory Tech. **47**(11), 2075–2084 (1999).
12. D. R. Smith, W. J. Padilla, D. C. Vier, S. C. Nemat-Nasser, and S. Schultz, "Composite Medium with Simultaneously Negative Permeability and Permittivity," Phys. Rev. Lett. **84**(18), 4184–4187 (2000).
13. S. Zhang, W. Fan, K. J. Malloy, S. R. Brueck, N. C. Panoiu, and R. M. Osgood, "Near-infrared double negative metamaterials," Opt. Express **13**(13), 4922–4930 (2005).
14. G. Dolling, M. Wegener, C. M. Soukoulis, and S. Linden, "Negative-index metamaterial at 780 nm wavelength," Opt. Lett. **32**(1), 53–55 (2007).
15. V. M. Shalaev, W. Cai, U. K. Chettiar, H. K. Yuan, A. K. Sarychev, V. P. Drachev, and A. V. Kildishev, "Negative index of refraction in optical metamaterials," Opt. Lett. **30**(24), 3356–3358 (2005).
16. O. Paul, C. Imhof, B. Reinhard, R. Zengerle, and R. Beigang, "Negative index bulk metamaterial at terahertz frequencies," Opt. Express **16**(9), 6736–6744 (2008).

#116926 - $15.00 USD Received 8 Sep 2009; revised 19 Oct 2009; accepted 19 Oct 2009; published 22 Oct 2009

17. M. Awad, M. Nagel, and H. Kurz, "Negative-index metamaterial with polymer-embedded wire-pair structures at terahertz frequencies," Opt. Lett. **33**(22), 2683–2685 (2008).
18. G. Donzelli, A. Vallecchi, F. Capolino, and A. Schuchinsky, "Metamaterial made of paired planar conductors: Particle resonances, phenomena and properties," Metamaterials (Amst.) **3**(1), 10–27 (2009).
19. A. Vallecchi, F. Capolino, and A. G. Schuchinsky, "2-D isotropic effective negative refractive index metamaterial in planar technology," IEEE Microw.Wireless Compon. Lett. **19**(5), 269–271 (2009).
20. J. Han, J. Gu, X. Lu, M. He, Q. Xing, and W. Zhang, "Broadband resonant terahertz transmission in a composite metal-dielectric structure," Opt. Express **17**(19), 16527–16534 (2009).
21. Z. Hao, M. C. Martin, B. Harteneck, S. Cabrini, and E. H. Anderson, "Negative index of refraction observed in a single layer of closed ring magnetic dipole resonators," Appl. Phys. Lett. **91**(25), 253119 (2007).
22. J. Zhou, E. N. Economon, T. Koschny, and C. M. Soukoulis, "Unifying approach to left-handed material design," Opt. Lett. **31**(24), 3620–3622 (2006).
23. D. Grischkowsky, S. Keiding, M. Exter, and C. Fattinger, "Far-infrared time-domain spectroscopy with terahertz beams of dielectrics and semiconductors," J. Opt. Soc. Am. B **7**(10), 2006 (1990).
24. A. K. Azad, J. M. Dai, and W. Zhang, "Transmission properties of terahertz pulses through subwavelength double split-ring resonators," Opt. Lett. **31**(5), 634–636 (2006).
25. X. Chen, T. M. Grzegorczyk, B. I. Wu, J. Pacheco, Jr., and J. A. Kong, "Robust method to retrieve the constitutive effective parameters of metamaterials," Phys. Rev. E Stat. Nonlin. Soft Matter Phys. **70**(1), 016608 (2004).
26. K. C. Gupta, R. Garg, and I. J. Bahl, Microstrip Lines and Slotlines, Artech House, 265 (1979).

1. Introduction

Negative index metamaterials (NIM) have attracted enormous interest in recent years due to their unique responses to electromagnetic radiation that were mostly not found in natural materials [1]. Such metamaterials have become an excellent platform for demonstrating unusual electromagnetic properties, thus leading to unique applications, such as superlens, cloaking, antenna, and sub-wavelength photolithography [2–10].

Although the concept of NIMs has existed for several decades, actual metamaterials were not experimentally demonstrated until recently. The original proposal and subsequent implementation for a practical NIM composed of conventional metallic wires, split-ring resonators (SRRs) and their variations [11]. The SRR-Wire composite was proved to be simultaneously negative in both permittivity and permeability with an overlapping electric and magnetic resonances [12]. In recent years, resonance frequencies of metamaterials have been extended from microwave to terahertz and visible regimes. Meanwhile, to improve the performance of metamaterials and to broaden their potential applications, numerous structures have been proposed and investigated either for in-plane or normal incidence [13–20], such as fishnet [13,14], rod pairs [15], crosses [16], and "dog bones" [17–19]. In addition to these structures, close-ring resonator has recently attracted researchers' attention for being an interesting candidate of metamaterial unit cell. In particular, negative index has been demonstrated at far infrared in a single-layer close ring metamaterial [21]. Compared to SRRs, the close rings have a two-dimensional (2D) symmetric character and less complicated fabrication processes. However, such structure only showed a negative index at in-plane incidence [21]. It is thus important to exploit its resonance properties at normal incidence, which is essential for three-dimensional (3D) metamaterial and device applications.

In this article, we present a freestanding metamaterial comprised of pairs of close rings resonating under normal wave incidence. The samples were fabricated by self-aligned photolithography on a flexible dielectric polymer. With terahertz transmission measurements, comprehensive model calculation, and a full-wave simulation, we demonstrate that the close-ring pair (CRP) geometry exhibits negative index of refraction at terahertz frequencies. Furthermore, we show that the electromagnetic response properties of the CRP structures can be efficiently controlled by varying their geometrical parameters.

2. Metamaterial structure

Figure 1(a) illustrates the schematic of a CRP unit cell. An h = 22 μm thick isotropic Mylar film is sandwiched between an aligned pair of square close rings of 200 nm thickness. Under electromagnetic radiation, the opposing ring pair, as well as the adjacent rings in the same plane form a composite LC-resonance circuit. Besides its 2D symmetric character, CRP was chosen as the unit cell because the coupling between adjacent rings in each plane of the CRPs

#116926 - $15.00 USD Received 8 Sep 2009; revised 19 Oct 2009; accepted 19 Oct 2009; published 22 Oct 2009

makes an additional and important contribution to their resonant properties [22], which is in contrast to the cut-wire pair structures. The samples were fabricated by a modified self-aligned lithography for double-layer process [4]. We chose commercially available Mylar film as the spacer because of its transparency in both terahertz and visible regime, thus enabling the unique self-aligned photolithography fabrication. Moreover, with a 22 μm thick Mylar spacer, the samples are not only freestanding but also flexible, which is very useful for many applications. The fabrication process is as follows: a layer of Al close rings was first patterned on Mylar by conventional photolithography using positive photoresist followed by metallization and lift-off process. The resulting ring pattern was subsequently used as a photo-mask to create an identical structure on the other side of Mylar with a negative photoresist, and followed again by lift-off process, thus establishing the final CRP structure.

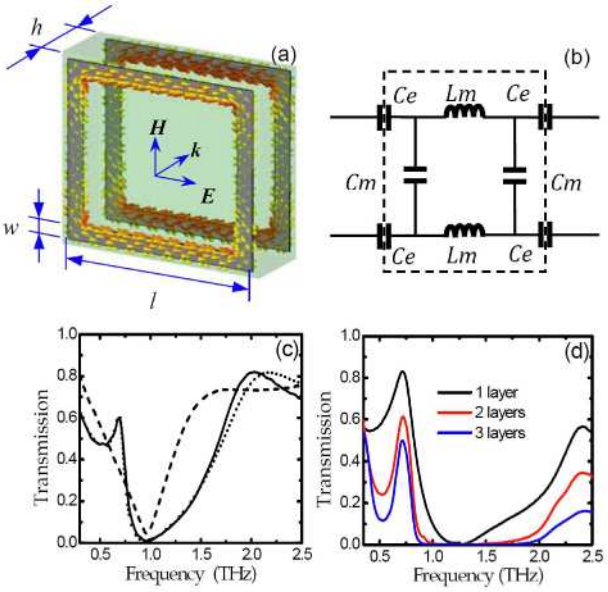

Fig. 1. (a) Schematic of a CRP unit cell with typical dimensions of l = 60 μm, w = 5 μm, and h = 22 μm. The arrows in the rings represent surface current induced at the resonance frequency. (b) Effective circuit model of the unit cell. (c) Measured (solid curve) and simulated (dotted curve) of a single-layer CRP metamaterial. The dashed curve illustrates the measured transmission of corresponding Al rings patterned only on one side of Mylar. (d) Measured transmissions of multi-layer CRPs. A Mylar film of 50 μm is used as the spacer in the multi-layer CRPs.

3. Transmission results and analysis

3.1 Experimental results and simulation

Transmission response of the CRP metamaterials was characterized under normal incidence using an photoconductive antenna based terahertz time-domain spectroscopy (THz-TDS) system [23,24]. The solid curve in Fig. 1(c) shows the frequency-dependent amplitude transmission of a CRP metamaterial with distance between two adjacent rings $d = 4$ μm. Compared to the ring array (dashed curve) patterned only on one side of Mylar, the CRP metamaterial reveals a new resonance peak at 0.69 THz while the stop-band valley near 1.0 THz becomes broader. Such resonant properties are well reproduced by numerical simulation (dotted curve). As shown in Fig. 1(a), the anti-symmetric current in the ring pair, induced by the incident magnetic field in the dielectric spacer, together with the displacement current between them form a loop and result in negative permeability at the resonance frequency. Thus, the combination of the negative permittivity, indicated by the wideband valley in the transmission response of a single layer of rings (dashed curve) in Fig. 1(c), and the negative permeability may lead to negative index of refraction near the resonance peak. With

#116926 - $15.00 USD Received 8 Sep 2009; revised 19 Oct 2009; accepted 19 Oct 2009; published 22 Oct 2009

increasing number of CRP layers, the peak resonance exhibits an improved contrast though the absolute transmission amplitude decreases due to material loss, as shown in Fig. 1(d). We note that the misalignment between the different CRP layers does not significantly influence the resonance behavior. Thus this poses a very robust design towards building a bulk metamaterial.

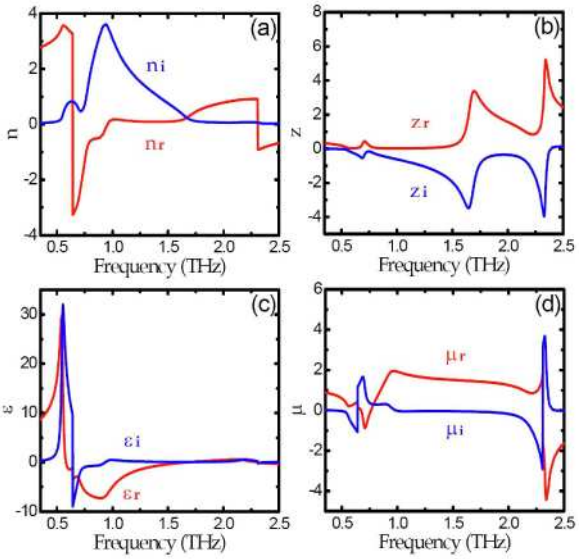

Fig. 2. Retrieved parameters of a single-layer CRP. The real and imaginary parts of the parameters are represented by the red and blue curves, respectively.

3.2 Parameters retrieval

Retrieval of the effective parameters requires the knowledge of the complex coefficients of both transmission and reflection. However, we could not obtain a faithful measurement of the reflection due to the flexible nature of our samples. Nevertheless, the almost perfect match between the measured and simulated transmissions (see Fig. 3) gives us the confidence to use the simulation results for the retrieval. Figures 2(a) and 2(b) shows the retrieved real and imaginary parts of the index of refraction n and the impedance z of the CRP metamaterial [16,25]. The *S11* and *S21* parameters were obtained by the simulation of a single layer of CRP sample with 25-μm air spacers both in front of and behind it. At 0.69 and 0.76 THz the index of refraction approaches −2.8 and −1.0, respectively. Figures 2(c) and 2(d) present the spectral behaviors of effective permittivity and permeability obtained through $\varepsilon_{eff} = n/z$ and $\mu_{eff} = nz$. Both ε_{eff} and μ_{eff} change dramatically around the resonance 0.69 THz and exhibit a distinct double negative behavior.

3.3 Analysis

To systematically explore the resonant behaviors of the CRP structure, we have fabricated a set of CRP metamaterials with various geometrical parameters. Apparently, modification in their geometrical dimensions results in extensive frequency shift and amplitude modulation at the resonance, as shown in Figs. 3(a), 3(c) and 3(e). The transmission peak blue-shifts with decreasing length of the ring l and increasing wire width w. With increasing periodicity (also the gap between the adjacent rings), the peak blue-shifts as well but becomes less pronounced.

#116926 - $15.00 USD Received 8 Sep 2009; revised 19 Oct 2009; accepted 19 Oct 2009; published 22 Oct 2009

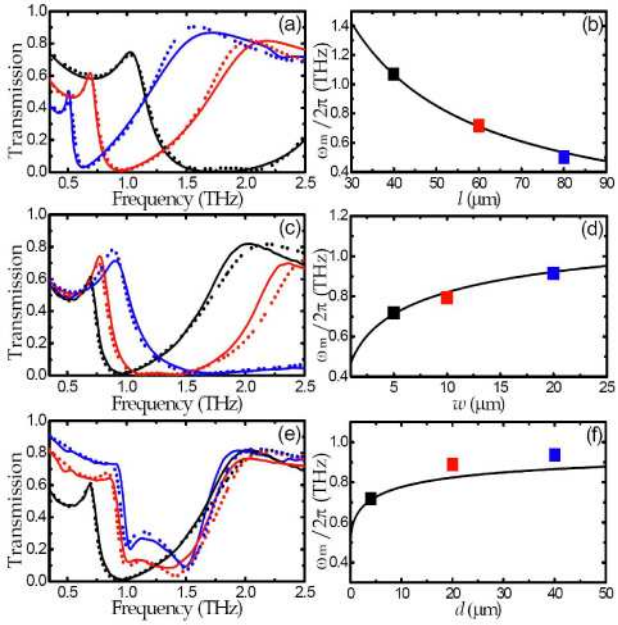

Fig. 3. Dependence of the CRP resonance on geometrical dimensions. (a), (c) and (e): measured (solid curves) and simulated (dotted curves) transmissions with (a) l = 40 (black), 60 (red) and 80 (blue) μm, (c) w = 5 (black), 10 (red) and 20 (blue) μm, and (e) d = 4 (black), 20 (red), and 40 (blue) μm, respectively. (b), (d) and (f): predicted (solid curves, by the circuit model) and simulated (squares) resonance frequencies.

According to surface current and electromagnetic field distribution, the resonance is largely determined by two factors: magnetic response between the two sides of CRP and the near field coupling between adjacent rings on the same side. In Fig. 1(b), we illustrate an effective circuit model of the CRP unit cell to further investigate the influence of geometrical parameters [22]. Here, the magnetic response is modeled by a microstrip loop across the two sides of the CRPs in the propagation direction and a coplanar line loop is used to represent the coupling between the adjacent rings at the same surface, respectively. The inductance and capacitance in the microstrips that are responsible for the magnetic response are denoted as L_m and C_m, respectively, while the capacitance C_e refers to the near field coupling coefficient between the adjacent rings on the same surface. The magnetic resonance frequency can be predicted as $\omega_m = \left[L_m\left(C_e + C_m\right)\right]^{-1/2}$, with $L_m = \mu hl/(2w)$, $C_m = \varepsilon w c_1 l/h$, $C_e = c_2 l(\varepsilon + \varepsilon_0)K\left(1-k^2\right)^{1/2}/\left[2K(k)\right]$, where ε and μ are the permittivity and permeability of the dielectric, in our case, $\varepsilon = 2.89\varepsilon_0$ and $\mu = \mu_0$; K is the first completed elliptical integration and $k = d/(d+2w)$ [26]; c_1 and c_2 are two numerical factors with values ranging between 0 and 1, which represent the effective length and width of the ring arms that really take part in the resonance, respectively. We find the best fits for the measurements are $c_1 = 0.31$ and $c_2 = 0.11$.

The decrease in l results in a linear decrease in L_m, C_m and C_e, thus explaining the blue-shift behavior shown in Fig. 3(a). The width w, as shown in Fig. 3(c), has an extensive effect on L_m, C_m and C_e with an overall result of blue-shifting the resonance frequency with increasing w. Figure 3(e) reveals the importance of the separation between the adjacent rings through its effect on C_e. In contrast to in-plane incidence, when the lattice dimension is increased, the resonance frequency is blue shifted and the peak is less pronounced [21]. In

#116926 - $15.00 USD Received 8 Sep 2009; revised 19 Oct 2009; accepted 19 Oct 2009; published 22 Oct 2009

Figs. 3(b), 3(d) and 3(f), we compare the simulated resonance position with that predicted by the circuit model and observe a reasonably good agreement.

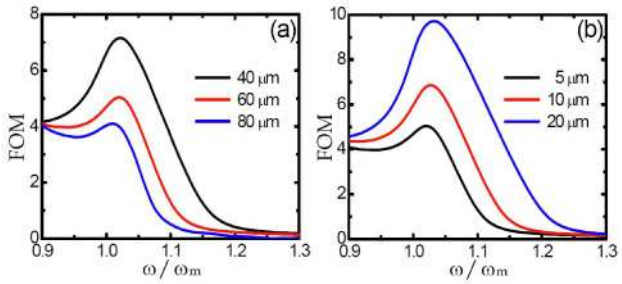

Fig. 4. Figure of Merit of the CRPs with various lengths (a) and wire widths (b). The x-axis is normalized to the resonance frequency.

3.4 Figure of merit

The figure of merit (FOM), $F = |n'/n''|$ of a passive component is an important measure that helps optimizing design for practical applications. Figures 4(a) and 4(b) illustrate the dependence of the FOM value on the length of the ring l and the width of wire w, respectively. The frequency axis is normalized to the resonance frequencies, $\omega_m/2\pi$. While l and w strongly influence the FOM, the periodicity or the gap between the adjacent rings is found to show much less effect. Namely, the FOM can benefit from a reduced length and an increased wire width. At $w = 20$ μm,a FOM of up to 9.72 is obtained, which is among the highest values for the existing terahertz metamaterials [16,17].

4. Conclusion

In conclusion, by use of self-aligned photolithography, THz-TDS, and numerical simulations, we demonstrate a freestanding negative-index metamaterial resonating at terahertz frequencies. Particular attention has been paid to the impact of geometrical parameters of the proposed unit cell on resonant behaviors and figure of merit. The flexible texture, straightforward fabrication process, and interesting resonant properties of the CRP geometries are promising in developing 3D terahertz metamaterials and metamaterial-based terahertz components.

Acknowledgement

The authors thank S. Zhang for stimulating discussions and exceptional help. This work was supported by the U.S. National Science Foundation, the National Key Basic Research Special Foundation of China (Grant Nos. 2007CB310403 and 2007CB310408), National Natural Foundation of China (Grant No. 60578037), and the Tianjin Sci-Tech Support Programs (Grant Nos. 08ZCKFZC28000 and 07ZCGHHZ01100). J. Han thanks financial support from the MOE Academic Research Fund of Singapore and the Lee Kuan Yew Fund.

#116926 - $15.00 USD Received 8 Sep 2009; revised 19 Oct 2009; accepted 19 Oct 2009; published 22 Oct 2009